CrystEngComm

Accepted Manuscript

ROYAL SOCIETY OF CHEMISTRY

www.rsc.org/crystengcomm

Journal Name

RSCPublishing

COMMUNICATION

Spontaneous Structure Transition in Nanoparticle Aggregates: From Amorphous Clusters to Super-crystals

Cite this: DOI: 10.1039/x0xx00000x

Received ooth January 2012,
Accepted ooth January 2012

DOI: 10.1039/x0xx00000x

www.rsc.org/

Xiaoshuang Shen,* Chao Mei, Hui He, Min Zhou, Weiwei Xia, Xianghua Zeng*

Spontaneous structure transition is an important process in the formation of normal crystals, which determines the structure and properties of final products. However, it is difficult to study this process in atom system experimentally. As an alternative, a detailed experimental study of this process in nanoparticle system is reported here.

It is believed that formation of long-order crystal structure is the most effective way to minimize the energy of a system containing infinite atoms or molecules at sufficiently low temperature. Recently, this opinion is further strengthened by the results from spherical nanoparticle (NP) system, in which spontaneous formation of a variety of super-crystals with the same structural symmetry of normal crystals has been demonstrated by numerous studies.[1-6] On the other hand, as known by people very early on, the minimum energy structure of a system containing finite building blocks is quite different. For example, the icosahedral structures with five-fold symmetry, which are incompatible to periodic crystals, were adopted by many kinds of atom or molecule clusters.[7,8] The icosahedral packing can maximize the number of contacts between spherical building units, and thus minimize the internal energy for some types of potential, such as the Lennard-Jones (LJ) potential.[9]

Since the structures of small clusters and corresponding bulk materials are intrinsically different, a structure transition definitely occurs during the growth process. However, our knowledge about when and how this transition happens is limited. The size of the clusters undergoing structure transition is somewhat too large for theoretical study even with the assistance of computers, which has been proved effective in study the minimum-energy structure of small clusters. The increased complexity in large clusters (containing thousands of or more atoms) makes the theoretical results highly depend on the approximation method applied, and thus controversial.[10] On the other hand, the size of the clusters is a little too small for the experimental study due to the difficulty in preserving and characterizing their structures, especially in single-cluster level. Recently, the method for preparation of NP clusters which possess similar structures with atom clusters was developed by several groups.[11-13] These highly stable NP clusters open an alternative way for addressing the issues about the structure transition in atom clusters.

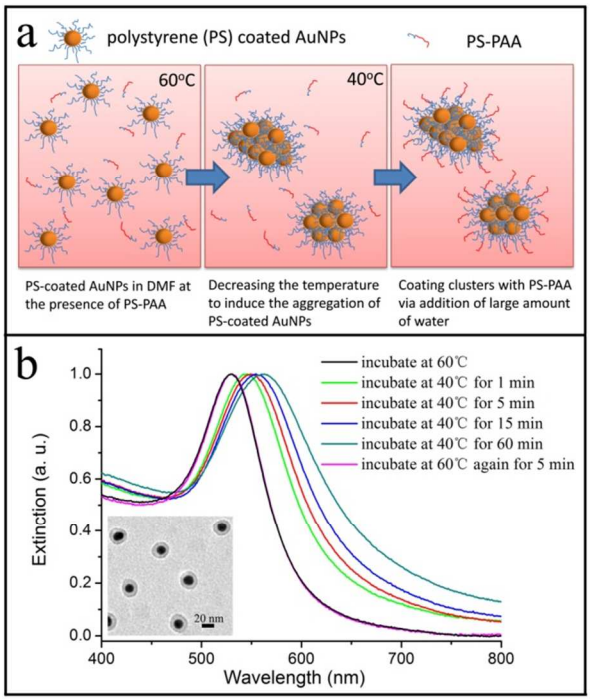

Figure 1. (a) Schematics of the experimental method. (b) Extinction spectra of the NP aggregates at different growth stage. The inset is a TEM image of the individual Au@PS NPs.

Here, we report an experimental study of the spontaneous structure transition in NP system. We observed the direct relation between the occurrence of structure transition and the size of NP aggregates. In our system, there is a small critical size ($d_{c.s}$) for this transition; all the NP aggregates with the size smaller than dc.s are amorphous. Similarly, there is a large critical size ($d_{c.l}$); all the NP aggregates with size larger than dc.l are crystalline. Detailed investigation of the super-crystal structures reveals that the structure transition starts from the outer-layer of the clusters and finishes at the center. In addition, control experiments with different building blocks show that formation of icosahedral structure in the small clusters is unfavorable for the structure transition.

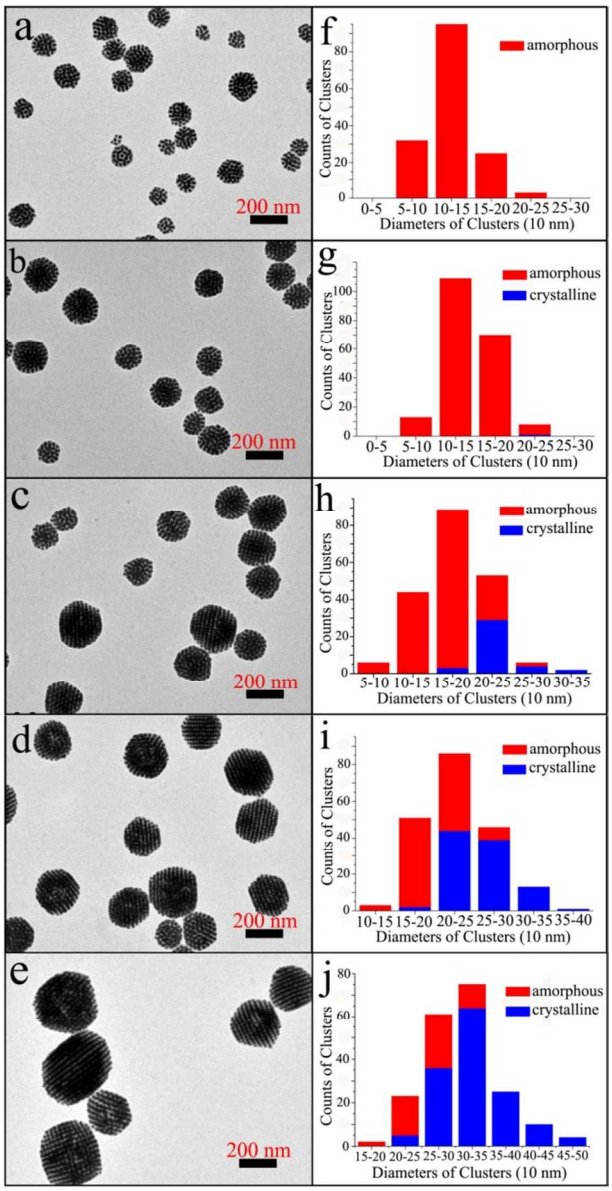

Figure 2. (a-e) TEM images of the clusters obtained at the growth time of 1, 5, 15, 60 and 240 min, respectively. (f-j) Size-distribution of the clusters obtained at the growth time of 1, 5, 15, 60 and 240 min, respectively.

The experimental method was illustrated in Figure 1a, and the details are given in the SI. We use Au@polystyrene(PS) core@shell nanoparticles as building blocks (inset of Figure 1b). The average diameter of Au cores was 15.2 nm. The shell is a mixture of two kinds of PS with average molecular weight (Mn) of 12k and 50k respectively. The mole ratio between the two polymers is about 2.5 : 1. Starting from a dimethylformamide (DMF) solution (~ 2 mL) containing well-dispersed Au@PS core-shell NPs and polystyrene-block-poly(acrylic acid) (PS-b-PAA, Mn = 1800 for PS and Mn = 6000 for PAA) at 60 ^{o}C, we add small amount of deionized water (42 μL) into the solution to increase the solvent polarity, which will decrease the stability of hydrophobic Au@PS NPs in it. Different from the method we developed previously for fabrication of small NP clusters,[13] here the amount of water is not enough to directly induce the aggregation of NPs. Then the solution was incubated at 40 ^{o}C to trigger the aggregation of NPs. As shown in Figure 1b, the peak in the extinction spectra shifts from 531 nm to 546 nm within 1 min, indicating the fast aggregation of NPs. The peak underwent further red-shift in the following 60 min, indicating the gradual size increase of the NP aggregates. It is worth pointing out that the aggregation of NPs here is reversible; the peak would shift back to 531 nm if we incubated the solution at 60 ^{o}C again for 5 min. To monitor the structural evolution of the clusters in the growth process, 100 μL of the solution was transferred into a 1.5-mL centrifugation tube at different time. Then 1 mL of deionized water was added to the tube to induce the encapsulation of PS-PAA on NP clusters.[14,15] The resulting aggregates were isolated and purified by centrifugation and redispersed in deionized water and then loaded on TEM grids.

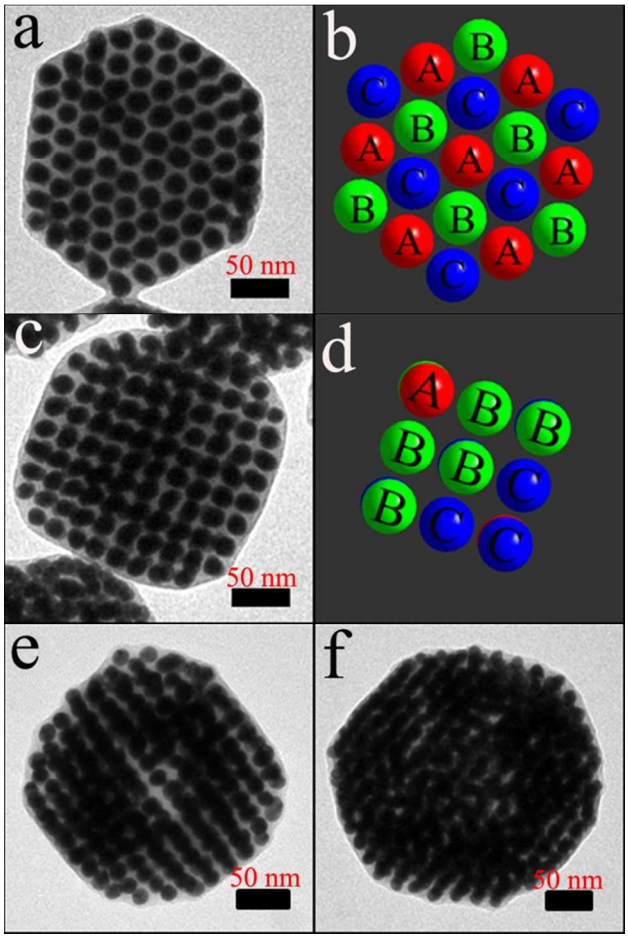

Figure 3. (a, b) TEM image and the corresponding schematic of a super-crystal viewed from <111> direction. (c, d) TEM image and the corresponding schematic of a super-crystal viewed from <100> direction. (e) TEM image of a super-crystal with a cavity in its center. (f) TEM image of a super-crystal with crystalline outer layer and amorphous center.

First, we focus our attention on the relation between the structure (amorphous vs. crystalline) and size of the aggregates. TEM images of the products obtained at 1, 5, 15, 60 and 240 min are given in Figure 2a-e (also see Figure S1), respectively. At 1 min (Figure 2a), all of the aggregates are amorphous with average size of ~ 128 nm. The sizes of the aggregates are all located within 50 to 250 nm (Figure 2f), and only 1.5% of the aggregates (200 surveyed, the same in the following cases) are found larger than 200 nm. At 5 min (Figure 2b), the average size of the aggregates increased to ~ 142 nm, and almost all of them remained amorphous. In the 200 aggregates we surveyed, only one aggregate with size located within the region of 200-250 nm is found to be crystalline (Figure 2g). At 15 min

(Figure 2c), the average size of the aggregates increased to ~ 171 nm, and 19% of the clusters are found to be super-crystals. All the super-crystals are larger than 150 nm, and the proportion of them are increased with cluster size (Figure 2h). At 60 min (Figure 2d), the average size and the proportion of super-crystals were increased to ~ 238 nm and 49.5%, respectively. The proportions of super-crystals in each size region are comparable in the cases of 15 min (Figure 2h) and 60 min (Figure 2i). The average size and the proportion of super-crystals can be further increased by prolonging the growth time. For example, at 240 min, NP aggregates with average size of ~ 260 nm were obtained (Figure 2e), and 72 % of them are super-crystals (Figure 2j).

The results discussed above clearly reveal the size-effect in spontaneous structure transition. All the small aggregates (< 150 nm) adopt the amorphous structure, which implies that formation of crystalline structure is not the effective way to minimize the system energy. The structure transition occurs in some aggregates when their size is larger than 150 nm. There is a competition between amorphous and crystalline structures for the aggregates with size between 150 and 300 nm, and the crystalline structure becomes overwhelming when the size is larger than 300 nm. The existence of $d_{c.s}$ (~ 150 nm, containing about 250 NPs) and $d_{c.l}$ (~ 300 nm, containing about 2000 NPs) clearly demonstrates the size-effect in the structure transition of NP aggregates.

The crystalline structure adopted by the NP aggregates is identified as face-centered cubic (fcc) structure, as shown in Figure 3a-d (also See Figure S2). Viewed from <111> direction, the NPs exhibit hexagonal close packing (Figure 3a and b), while from <100> direction, they exhibit square packing (Figure 3c and d). In the schematic diagrams given in Figure 3b and d, the balls with the same colour represent the Au NPs in the same hexagonal close packing layer, and the gap between the neighbouring same-colour balls is due to the polymer shells (~ 8.6 nm, corresponding to ~ 17.2 nm gap. See Figure S3) on Au NPs, which is almost transparent under TEM.

The fact that the fcc structure has the highest packing density (~ 0.74) for spherical building units provides a clue for explaining an interesting phenomenon you may have noticed in Figure 2d and e. Some super-crystals (~ 50%) have a "hollow" structure, according to the contrast between the center and outer layer of these super-crystals. An enlarged TEM image of a hollow super-crystal is given in Figure 3e, in which a cavity appears clearly at the center. The cavity seldom appears in the amorphous aggregates, so the formation of it should be related to the structural transition, and not due to other reasons such as the bubbles in the solution.[16] We also noticed a few of special NP aggregates; their outer layer exhibits a crystalline structure, while their center is amorphous (Figure 3f). This structure can be looked as intermediate state of a NP aggregate under structure transition, which implies that the structure transition starts from the outer layer, and gradually proceeds into the center. In other words, it is a surface driven crystallization predicted in atom system.[17,18] According to this mechanism, the local stable (111) regions formed on the surface provide a template for the ordering the core regions. In our case, once a crystalline outer layer is formed, the inner NPs will adjust their arrangement and add to the outer layer with *fcc* packing. Since the *fcc* structure has the highest packing density, a cavity will appear at the center after the transition from amorphous (lower packing density) to *fcc* structure. The cavity is a kind of defect for an ideal super-crystal, so there will be a driving force to remove this defect to reach the most stable structure by rearranging the NPs. This is the possible reason why the cavity is absent at some super-crystals.

In atom system, the structure transition is highly related to the interaction between atoms.[9] For the Au@PS core-shell NPs, the interaction between them is mainly determined by the hydrophobic PS shells; it can be easily tuned by changing the PS chains. Instead of using two kinds of PS with average molecular weight (Mn) of 12k and 50k in the above experiments, a control experiment with only PS of 12k was performed. In this case, the shell thickness is about 3.9 nm (inset of Figure 4a). The smaller gap between Au NPs leads to stronger plasmonic coupling and a new peak located around 650 nm appears in the extinction spectra of NP aggregates (Figure 4a). The average size of NP aggregates obtained at 60 min is about 326 nm, larger than the $d_{c.l}$ observed in above experiments, but all of the aggregates are still amorphous (Figure 4b and Figure S4). The expected structure transition did not occur in this case.

The structural differences in the products of the two experiments can be traced back to the initially formed NP clusters. Figure 4c shows the TEM images of the products obtained at 1 min in the control experiment. The structure of the small clusters follows the icosahedral scheme (Figure 4d-i, and Figure S5). Starting from a decahedron (Figure 4d and e, containing 7 NPs), which can be looked as an uncompleted icosahedron, the following clusters are formed by adding NPs on the faces of the decahedron until a completed icosahedraon (Figure 4f and g, containing 13 NPs) is formed. Similarly, larger clusters can be formed by adding NPs on the faces of the icosahedron (Figure 4h and I, containing 16 NPs). In the clusters containing hundreds of NPs, local icosahedral structure can be easily identified (Figure 4j). In the previous experiments with two kinds of PS, the structures of the small clusters are quite different. The majority of the products are not icosahedral clusters (Figure 2a). Two small clusters are imaged in Figure 4k and l, and obviously, their structures do not follow the icosahedral scheme.

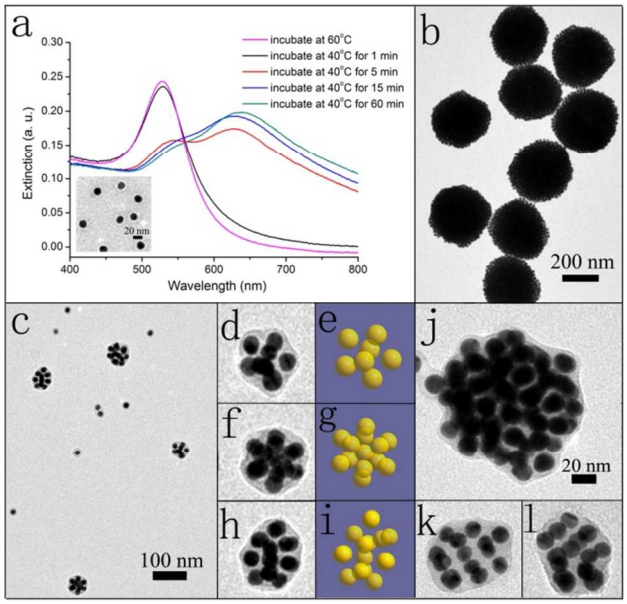

Figure 4. (a) Extinction spectra of the NP aggregates. The inset is a TEM image of the individual Au@PS NPs with thin PS shells. (b) TEM images of the products obtained with only PS of 12k. (c) TEM images of the products obtained at 1 min. (d – i) Enlarged TEM images and corresponding structural diagrams of three small clusters in (c). (j) TEM image of a large cluster with local icosahedral packing. (k –l) TEM images of two small clusters (containing 13 and 14 NPs respectively) obtained in previous experiments with thick PS shells.

The structural differences of the small clusters in the two cases can be well explained by considering the differences in the PS shells. In the control experiment, only short-chain PS (Mn: 12k) was used. The introducing of small amount of long-chain PS (Mn: 50k)

increased the range of interaction between NPs (for further discussion, see Figure S6). It is known that short-range interaction, such as the one described by LJ potential, favors the formation of icosahedral structures, which maximize the number of contacts between building units. For long-range interaction, the contribution from the interaction between noncontact particles makes some other structures comparable in energy with the icosahedral structures. In addition, the fact that three-dimensional space cannot be filled with tetrahedra leads to some inevitable deformation in the icosahedral structures (Figure S7), and thus high strain energy exists in these structures. The strain energy increased quickly with increasing the range of interaction, which will destabilize the icosahedral structures.[19] In the control experiment, formation of clusters with icosahedral or local icosahedral structures is quite favorable. The fivefold symmetry in these structures has been called as an inhibitor to crystallization,[20] which inhibits the structure transition.

Conclusions

In summary, the spontaneous structure transition was studied in a real NP system. Our study confirms the size-effect in this transition, and also reveals that the transition starts from the outer layer of the NP aggregates and finishes at the centre. The control experiment shows that the interaction between NPs determines the structures of small clusters, which has a great influence on the structure transition. These observations will not only promote our understanding of the spontaneous structure transition in atom system, but will benefit our control on the structure and thus the properties (e.g., photothermal effect) of NP clusters.[21-23]

Notes and references

School of Physical Science and Technology & Institute of Optoelectronic Technology, Yangzhou University, Yangzhou 225002, P. R. China
* Corresponding author. E-mail:
xsshen@yzu.edu.cn; xhzeng@yzu.edu.cn.

Acknowledgements

The work was funded through the Natural Science Foundation of the Jiangsu Higher Education Institutions of China (No. 14KJB150028), the Innovation Fostering Foundation of Yangzhou University (2014CXJ010) and Natural Science Foundation of China (No. 61474096, 51301152, 61301026). The authors thank Professor Hongyu Chen in NTU for helpful discussion.

Electronic Supplementary Information (ESI) available: Details of procedures, methods, and large-area views of TEM images. See DOI: 10.1039/c000000x/

1 A. M. Kalsin, M. Fialkowski, M. Paszewski, S. K. Smoukov, K. J. M. Bishop and B. A. Grzybowski, *Science,* 2006, **312**, 420.
2 T. Wang, J. Zhuang, J. Lynch, O. Chen, Z. Wang, X. Wang, D. LaMontagne, H. Wu, Z. Wang and Y. C. Cao, *Science,* 2012, **338**, 358.
3 H. Wang, L. Chen, Y. Feng and H. Chen, *Acc. Chem. Res.*, 2013, **46**, 1636.
4 Y. Wang, J. He, C. Liu, W. H. Chong and H. Chen, *Angew. Chem. Int. Ed*, 2015, **54**, 2022.
5 A. Pal, V. Malik, L. He, B. H. Erne, Y. Yin, W. K. Kegel and A. V. Petukhov, *Angew. Chem. Int. Ed*, 2015, **54**, 1803.
6 Z. Qian, S. P. Hastings, C. Li, N. Engheta, Z. Fakhraai and S. Park, *ACS Nano*, 2015, **9**, 1263.
7 A. Das, T. Li, K. Nobusada, Q. Zeng, N. L. Rosi and R. Jin, *J. Am. Chem. Soc*, 2012, **134**, 20286.
8 J. Farges, M. F. Feraudy, B. Raoult and G. Torchet, *J. Chern. Phys*, 1983, **78**, 5067.
9 J. A. Northby, *J. Chem. Phys,* 1987, ***87***, 6166.
10 B. Hartke, *Angew. Chem. Int. Ed,* 2002, **41**, 1468.
11 A. Sanchez-Iglesias, M. Grzelczak, T. Altantzis, B. Goris, J. Perez-Juste, S. Bals, G. V. Tendeloo, S. H. Donaldson Jr, B. F. Chmelka, J. N. Israelachvili and L. M. Liz-Marzan, *ACS Nano,* 2012, **6**, 11059.
12 J. Lacava, P. Born and T. Kraus, *Nano Lett*, 2012, **12**, 3279.
13 A. Urban, X. Shen, Y. Wang, N. Large, W. Hong, M. W. Knight, P. Nordlander, H. Chen and N. J. Halas, *Nano Lett*, 2013, **13**, 4399.
14 T. Chen, M. Yang, X. Wang, L. H. Tan and H. Chen, *J. Am. Chem. Soc,* 2008, **130**, 11858.
15 L. Zhu, H. Wang, X. Shen, L. Chen, Y. Wang and H. Chen, *Small,* 2012, **8**, 1857.
16 J. He, Y. Liu, T. Babu, Z. Wei and Z. Nie, *J. Am. Chem. Soc*, 2012, **134**, 11342.
17 G. Opletal, C. A. Feigl, G. Grochola, I. K. Snook and S. P. Russo, *Chem. Phys. Lett,* 2009, **482**, 281.
18 Y. H. Chui, R. J. Rees, I. K. Snook, B. O'Malley and S. P. Russo, *J. Chem. Phys,* 2006, **125**, 114703.
19 J. P. K. Doye, J. David and D. J. Wales, *J. Chem. Phys,* 1995, **103**, 4234.
20 N. C. Karayiannis, R. Malshe, J. J. de Pablo and M. Laso, *Phys. Rev. E,* 2011, ***83***, 061501.
21 C. Yang, H. Sui, X. Li, J. Han, X. Luo, H. Zhang, H. Sun, H. Sun, Y. Zhou and B. Yang, *CrystEngComm*, 2013, **15**, 3490.
22 X. Zhang, M. Lin, X. Lin, C. Zhang, H. Wei, H. Zhang and B. Yang, *ACS Appl. Mater. Interfaces*, 2014, **6**, 450.
23 X. Zhang, X. Xu, T. Li, M. Lin, X. Lin, H. Zhang, H. Sun and B. Yang, *ACS Appl. Mater. Interfaces*, 2014, **6**, 14552.

